Iranian Journal of Science and Technology, Transactions of Civil Engineering (2022) 46:2449–2467
https://doi.org/10.1007/s40996-021-00787-5

RESEARCH PAPER

Effect of the Shape and Position of the Bridge Pier on the Bed Changes in the Sharp 180-Degree Bend

Arsalan Keshavarz[1] · Mohammad Vaghefi[1] · Goodarz Ahmadi[2]

Received: 25 December 2020 / Accepted: 7 November 2021 / Published online: 15 November 2021

Abstract

This paper has experimentally investigated the simultaneous effect of the pier shape and position on scouring in a sharp 180-degree bend. Several experiments were performed on the bend for nine different pier shapes at three different positions, and the corresponding shape factors coefficients (ratio of maximum scour depth to that of a circular pier) were evaluated for all pier shapes at each position. The presented results show that the shape factor coefficient (Ks) is mostly affected by the pier geometric shape and the effect of position of the piers is small. Furthermore, the piers with low width and sharp nose create shallow and low-volume scour hole. In contrast, deeper holes are created around the piers with wide nose and sharp edges with larger volumes. Also, the results showed that the maximum scour depth is equal to 4.22 times the pier width in the case of rectangular pier located at 90-degree bend position and the lowest scour is equal to 2.12 times the pier width that was created around the jou.sharp pier located at the 120-degree bend position. The maximum scour depth for the jou. sharp pier installed at the 120-degree position has decreased by 50% compared to that for the rectangular pier placed at the 90-degree position.

Keywords 180-degree bend · Pier shape · Pier position · Scour · Shape factor

List of symbols

B	Channel width
b	Distance from inner bank
D	Width of the pier
D.S	Slope of hole toward downstream
Ds	Scour depth
d_{16}	Grain size for which 16% by weight of the sediment is finer
d_{84}	Grain size for which 84% by weight of the sediment is finer
hs	Sedimentation height
I.S	Slope of hole toward inner bank
Ks	Shape factor
L	Length of the pier
Lms	Length of sedimentation motion
O.S	Slope of hole toward outer bank
R	Central radius of the bend
S	Maximum length of the scour hole
U.S	Slope of hole toward upstream
V	Scour hole volume
W	Maximum width of the scour hole
σ_g	Geometric standard deviation of sediment grading

1 Introduction

Bridge pier scour has always been a concern for civil engineers as one of the most important factors in the destruction of bridges. The interaction of flow stream with the pier causes the formation of a horseshoe vortex around the pier and wake vortices behind the pier. The downflow component which attacks the bed in return will lift up the sediments. The sediments are trapped in the horseshoe vortex and transported to the downstream. The particles at the back of the pier are lifted by the action of uprising vortex.

✉ Mohammad Vaghefi
Vaghefi@pgu.ac.ir

Arsalan Keshavarz
Arsalan.keshavarz2011@gmail.com

Goodarz Ahmadi
gahmadi@clarkson.edu

[1] Department of Civil Engineering, Persian Gulf University, Shahid Mahini St., 7516913798 Bushehr, Iran

[2] Mechanical and Aeronautical Engineering Department, Clarkson University, 8 Clarkson Ave, Potsdam, NY 13699, USA

There have been several recent studies on scour around bridge piers that are briefly outline in this section.

Akib et al. (2014) conducted an experimental study of scour mechanism and flow pattern around semi-integral group bridge piers. The results indicated that increasing the flow depth and the discharge resulted in an increase in scour. Velocity distribution also influences scour. Ismael et al. (2015) studied the scour around "circular," "upstream facing round-nosed," and "downstream facing round-nosed" piers with different upstream and downstream nose widths. Their results indicated that by using the "downstream facing round-nosed" pier, the maximum scour depth reduces by 54 and 40% in comparison with "circular" and "upstream facing round-nosed" piers, respectively. Moreno et al. (2016) studied scour around the bridge pier located on a pile-cap experimentally. In this work, different ratios of pile-cap thickness to pier thickness at different levels of pile-cap in proportion to base level were tested, and the effect of these on scour for three pile-cap positions (above bed level, partially in the bed, and fully under the bed) was investigated, and it was observed that the maximum scour depth occurred with the partial placement of the pile-cap in the bed. Wang et al. (2016) carried out an experimental investigation of scour around double circular bridge piers in a straight path. The results demonstrated that the scour hole created around the upstream pier is similar to the scour hole around the single pier under the same conditions, whereas the scour depth around the pier downstream is lower than that at the pier upstream. Yagci et al. (2017) examined different arrangements of a group of 6 piers in regular, angled, and staggered configurations at various distances. Their results suggested that using these arrangements could reduce the volume of scour hole by 27% and the depth of scour hole by 22% in comparison with a single pier case. Baghbadorani et al. (2017) analyzed experimental data that complied from previous studies and compared the results with those obtained from available empirical equations. They also proposed a new formula that reduces the error by 10%. Khaple et al. (2017) studied scour around circular piers with three kinds of pier arrangements. These are (i) two piers in tandem, (ii) two piers in staggered arrangements, and (iii) three piers in symmetrically staggered arrangements. Their results indicated that in the arrangements of two piers in tandem, the equilibrium scour depth decreases with an increase in the downstream distance up to approximately eight pier diameters and then increases with further increase in the downstream distance. Yang et al. (2018) examined the local scour around complex bridge piers at two typical pier models, nine different pile-cap elevations and seven different pier skew angles under clear water conditions. Wang et al. (2018) studied the influence of a submerged weir, located at the downstream side of a circular bridge pier at different distances from the pier, on the local scour around the pier under clear water and live bed conditions. Keshavarzi et al. (2018) inspected the scour around twin circular bridge piers aligned in the flow direction for different distances of the piers from each other under clear water conditions. Tipireddy and Barkdoll (2019) investigated the effect of air injection on scour reduction around a single circular bridge pier under clear water condition and considered different ratios of air velocity to water velocity. Galan et al. (2019) inspected the effects of the skew angle, submergence ratio, and pile group configuration on the scour around grouped bridge piers in two different arrangements. Karimaei Tabarestani and Zarrati (2019) examined the scour around a circular bridge pier equipped with a collar under steady and unsteady conditions with different U/Uc values. Lee and Hong (2019) addressed the flow pattern prior to and following scour around a bridge pier. Measurements indicated that the flow velocity values at the upstream side of the pier, where horseshoe vortices are generated, are greatly different before and after the scouring. Chavan et al. (2019) investigated the scour around a single circular bridge pier with no seepage and with downward seepage. Carnacina et al. (2019) studied the scour around a circular bridge pier under pressure flow conditions. Das et al. (2019) conducted an investigation of the scour around triad circular bridge piers placed at different distances from each other. Namaee and Sui (2019) investigated the local scour around four pairs of side-by-side circular bridge piers under ice-covered flow conditions. Wang et al. (2019) examined the function of an anti-scour collar at different levels, dimensions, and collar protection ranges around a cylindrical pier. Yang et al. (2019a, b) addressed the scour around grouped bridge piers in four different arrangements under clear water and live bed conditions. Memar et al. (2020) considered the effect of the collar diameter and level on scour reduction around twin circular bridge piers. Laxmi Narayana et al. (2020) investigated the scour hole around single and twin circular bridge piers under different flow conditions. Malik and Setia (2020) examined scour around twin and triad circular piers in tandem, side by side, and staggered arrangements. Link et al. (2020) studied local scour and sedimentation during flood waves around the Rapel Bridge located over the Rapel River. Yang et al. (2020) conducted a study of scour around grouped bridge piers with a streamwise arrangement or at skew angles with the flow direction under clear water conditions.

One of the important parameters affecting the process of scouring is the geometric shape of pier. The shape factor K_s is the ratio of maximum scour depth around each pier to the maximum scour depth around the circular pier. A number of previous researchers have done research on the shape factor. Diab (2011) presented a summary of the shape factors obtained by previous researchers.

Additional research has also been done on the effect of geometric shape of piers in recent years. For a straight

river segment, Fael et al. (2016) studied the effect of the pier shape and its placement angle on the scour depth of the single bridge in a straight channel. In these experiments, five different types of piers were tested. They found a shape factor of 1 for the rounded corner rectangular piers and a shape factor of 1.2 for the sharp corner rectangular piers. Al-shukur and Obeid (2016) studied the effect of pier shape on scour in a straight channel. Ten different pier shapes were examined in this study. Farooq and Ghumman (2019) investigated scouring around six different pier shapes in an experimental channel with a straight path. Vijayasree et al. (2019) studied the flow pattern and local scour around five different shapes of bridge piers under the same flow conditions. Yang et al. (2019a, b) carried out a study on the scour around skewed rectangular and circular piers under live bed conditions.

It should be emphasized that all previous studies on the shape factor were conducted in straight channels. However, most rivers have meandering paths, and the stream flows in bends lead to secondary flows, which cause erosion of the outer bank and sedimentation adjacent to the inner bank. Therefore, for bridges at the river bends, in addition to the formation of horseshoe and wake vortices, the scroll flows also affect the scouring process. In the past, a number of researchers have studied the role of the bridge pier in changing the flow pattern and scouring in the river bends.

Masjedi et al. (2010) examined the effect of placement of a rectangular bridge pier on the scouring rate in a 180-degree bend with a relative curvature radius (ratio of bend radius to channel width) equal to 4.67. The results of their experiments showed that the maximum scour depth occurs for the pier placement angle at 60-degree, and the scour depth increases with increasing Froude number. Ben Mohammad Khajeh et al. (2017) conducted an experimental study of an inclined circular pier in the 180-degree sharp bend. The results indicated that the minimum scour depth was 0.7 times the flow depth in the upstream straight channel and occurred at the pier inclined toward the inner bank. The maximum scour depth was 1.05 times the flow depth at the upstream straight path, and it occurred at the pier inclined toward the outer bank. Vaghefi et al. (2018) examined scour patterns around triad circular section piers perpendicular to flow and piers toward the flow at different sections of a 180-degree bend in a flume. The results showed that the maximum scour depth around the piers was equal to 1.1 times the flow depth at the beginning of the bend and the maximum sedimentation height was equal to 0.7 times the flow depth at the beginning of the bend and was observed at 156-degree position of the bend at a 20% distance of the flume width from the inner bank and both occurred for the case of piers placed perpendicular to the flow at 90-degree position. Moghanloo et al. (2020a) investigated the effect of collar thickness and level on scouring around an oblong pier in a 180-degree sharp bend. Moghanloo et al. (2020b) inspected the effect of thickening a collar on the flow pattern around an oblong pier implemented at the 90-degree angle of a 180-degree sharp bend. Dehghan et al. (2021a) studied different sizes of an oblong pier located at the 90-degree angle of a 180-degree sharp bend as well as the angle of impact of the flow and the pier and the effects of these two parameters on scour. Dehghan et al. (2021b) explored the effect of collar width on the flow pattern round an oblong pier installed at the 90-degree angle of a 180-degree sharp bend. The results demonstrated that using the collar led to power shrinkage of power reduction in downflows in the vicinity of the pier and increasing the collar width resulted in a reduction in vorticity and the power of the secondary flows.

The presented brief review of the earlier works suggests that the shape of the bridge pier section and its position in the bend are two important parameters affecting the pier scouring. In this paper the scours around various bridge pier shapes located at different positions in a 180-degree bend were investigated. The minimum and maximum scour depths and sediment heights, the volume of scour holes, and the slope of scour holes were experimentally evaluated. The topographic changes of the channel bed were also investigated. In addition, the values of shape factors for different shape piers at various sections of the bends were evaluated.

2 Materials and Methods

Experiments were carried out in a channel with 180-degree bend. Figure 1 shows the channel. The channel has a rectangular cross section with a width of 1 m and a height of 70 cm. The upstream and downstream of the bend are straight parts with lengths of respectively 6.5 m and 5 m. The radius of the central curvature of the bend of the channel is 2 m. This channel with R/B = 2 falls into the category of sharp bends, where R is the central radius of the bend and B is the channel

Fig. 1 The laboratory channel used

width. According to Melville and Chiew (1999), the particle diameter size must exceed 0.6 mm in order to prevent ripple formation. To this end, in this laboratory, particles with an average diameter of 1.5 mm and a standard deviation of 1.14 [$\sigma_g = (d_{84}/d_{16})^{0.5} = 1.14$] have been used where d_{84} and d_{16} are grain sizes for which 84 and 16% by weight of the sediment is finer, respectively. All experiments have been carried out in conditions close to the threshold of incipient motion in the upstream straight path of the bend with the ratio of mean flow velocity to critical velocity (U/Uc) of 0.98. The flow rate of 0.07 cubic meter per second (M^3/S) and the water depth of 18 cm were selected for the experiments. Froude and Reynolds numbers are 0.3 and around 50,000, respectively.

Rectangular, circular, oblong, joukowsky sharpnose, joukowsky roundnose, elliptical, hexagonal, octagonal, and sharpnose shapes for the pier section were used in the experiments (Fig. 2). According to Chiew and Melville (1987), to eliminate the effect of banks on local scour around the pier, the pier diameter should not exceed 10% of the channel width. Further, the pier's optimum ratio of length to width is between 3 and 5 (Dehghan et al. 2021a). Therefore, piers with width of 5 and length of 20 cm ($L/D = 4$) were used in these experiments. Here L is the length and D is the width of the pier. Each pier was tested at positions 60, 90, and 120 degrees. According to the results of Vaghefi et al. (2016), the maximum vorticity and shear stress values in the test on the 180-degree sharp bend without piers occurred within the range of 40–60 degrees. Therefore, the 60-degree angle was selected as one of the angles to be investigated. Further, in order to analyze scouring in the second half of the bend as well, the 120-degree angle was selected due to its symmetry with the 60-degree angle. The 90-degree angle was also studied because of its position at the bend apex.

It should be noted that the joukowsky pier is placed in the direction of flow once from the rounded nose (jou.round) and once from the sharp nose (jou.sharp), and thus nine different shapes of the bridge pier have been used in this study. In the first step, in order to determine the relative equilibrium time for conducting the experiments, a 34-h equilibrium test with an oblong pier located at 90 degrees of bend was performed. In the time-equilibrium test, the increase in the maximum scour depth was measured continuously with time. It was observed that approximately 95% of the maximum scour occurred in the first 15 h of the test. Measurement continued until there was not noticeable change in maximum scour depth at three consecutive 4-h intervals. So, according to the criterion of Chiew (1992), the time of 15 h was selected as the relative equilibrium time for the subsequent experiments.

After determining the relative equilibrium time, a test was conducted to study the bed topography changes in the bend without pier that is bend without placement of the pier in the flow path. The purpose of this experiment is to determine the behavior of bend without hydraulic structures and under the influence of the flow conditions in the bend. The corresponding bed height contours after 15 h are shown in Fig. 3.

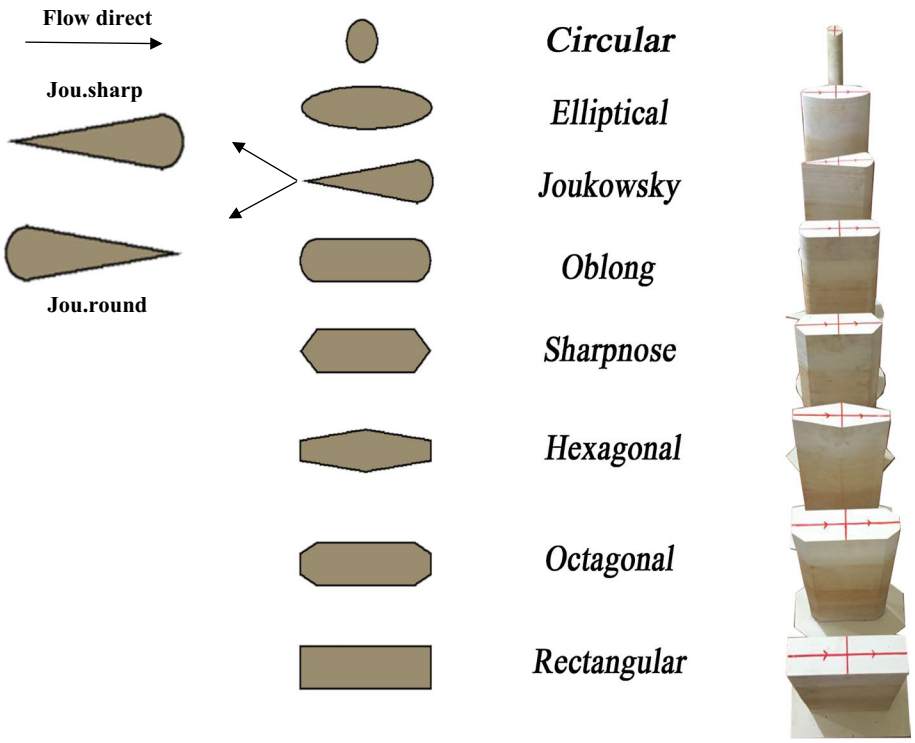

Fig. 2 Schematics of pier cross section studied

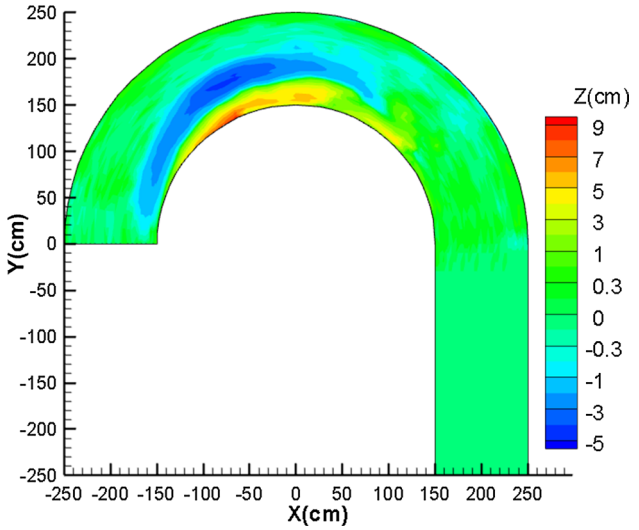

Fig. 3 Bed topography changes in the test of the empty bend without piers

As observed in Fig. 3, the topography of the bed in the bend varies due to the presence of spiral streams with sedimentation on the inner bank and erosion in the middle. It is also observed that the sedimentation adjacent to the inner bank began at 35-degree and continued to 145-degree. The maximum sedimentation of 8.7 cm occurred at an angle of 65-degree (equivalent to 0.48 times the depth of the water in the upstream straight path). Scouring also starts from the angle of 10-degree and continues to 120-degree. The maximum scouring of 4.2 cm (equivalent to 0.23 times the depth of the water in the upstream straight channel) occurs at the angle of 65-degree.

3 Results and Discussion

The main objective of this paper is to provide the effect of position of different bridge shapes on the scour around the pier and the bed topography. For this purpose, nine different pier shapes were tested at 60, 90, and 120 degrees. A summary of the results is presented in Table 1.

As shown in Table 1, the maximum and minimum scour depths in each of the three positions are, respectively, associated with the rectangular and jou.sharp pier placement. The maximum scour depth is equal to 4.22 times the pier width in the case of rectangular pier at 90-degree and the lowest scour is equal to 2.12 times the pier width in the jou. sharp pier at the angle of 120-degree. Moreover, as shown in the results of Dehghan et al. (2021a), the maximum scour depth was observed around an oblong pier with a ratio of length to width equal to 6 and placed at the 90-degree, and the minimum scour depth occurred around an oblong pier with a ratio of length to width equal to 2 and placed at the 120-degree angle.

It is also observed that for all the piers, except for the jou.sharp pier, the maximum scouring occurs in the vicinity of the upstream nose of the piers. However, the maximum scour depth in the case of jou.sharp pier was in the vicinity of the downstream nose of the pier. The reason is that due to the sharp tip of the upstream nose and the round shape of downstream nose in the jou.sharp pier, the separation of the flow occurs more around the downstream nose of the pier and the flows formed are more downward. For this reason, the maximum scouring occurred on the pier downstream.

The pier nose's aerodynamic shape plays a considerable role in reducing scour around the pier. This has also been observed in research conducted by Al-Shukur and Obeid (2016). The results of Al-Shukur and Obeid (2016) indicated rectangular and streamline piers to, respectively, have the maximum and the minimum scour depths. In addition, according to Farooq and Ghumman (2019), the octagonal pier they utilized in their study was the most efficient in reducing scour among all their piers.

According to Table 1, it is obvious that for all piers, the maximum sedimentation height in pier placement of 60-degree is higher than the placement at 90- and 120-degree. This is also comparable to the results obtained by Dehghan et al. (2021a), where the maximum sediment height for every pier with different ratios of length to width was greater at the 60-degree position of the piers than that for the same piers at 90 and 120-degree positions.

Among the piers located at 60-degree of bend, the maximum sedimentation height is equal to 2.3 times the pier width and is related to the hexagonal pier placement. This sedimentation occurs at an angle of 115-degree, at a distance of 1% of the channel width from the inner bank. Among the piers located at the angle of 90-degree of bend, the maximum sedimentation height is equal to 1.98 times the pier width and on the downstream of the circular pier (angle of 165 degrees). In the case of pier placement at the angle of 120-degree, the highest sediment height is equal to 1.78 times the pier width on the upstream of the octagonal pier (73-degree angle) and adjacent to the inner bank.

As for the scour hole volume, as well as the maximum depth of scour hole, the maximum and minimum scour hole in each of the three positions occurs for the rectangular and jou.sharp piers, respectively. The maximum volume of the hole is equal to 236.6 times the third power of the pier width ($V/D^3 = 236.6$) around the rectangular pier at the 60-degree angle (Fig. 4a) and the minimum volume is equal to 30.6 times the third power of the pier width ($V/D^3 = 30.6$) around the jou.sharp pier located at 120-degree angle (Fig. 4c).It was also observed in Dehghan et al. (2021a) that the maximum scour hole volume equal to 209 times the third power of the pier width ($V/D^3 = 209$) occurred with the oblong pier

Table 1 Summary of experimental results

No.	Pier's shape	Position	Scour			Sedimentation					
			dsmax/*D*	At		hsmax/*D*	at		V/D^3	*L*ms/*D*	K_s
				Θ	*b/B*		Θ	*b/B*			
1	Circular	60°	3.14	60°	0.48	2.1	110°	0.01	141.6	77.5	1
2	Elliptical	60°	3.64	57°	0.5	1.98	115°	0.01	175.1	71.9	1.2
3	Jou.sharp	60°	2.44	63°	0.53	2.06	115°	0.01	86.4	59.3	0.8
4	Jou.round	60°	3.5	57°	0.53	2.1	110°	0.01	171.2	70.5	1.1
5	Oblong	60°	3.4	57°	0.5	1.84	125°	0.01	175.8	69.8	1.1
6	Sharpnose	60°	2.82	57°	0.5	1.78	115°	0.01	91.2	52.3	0.9
7	Hexagonal	60°	3.38	57°	0.53	2.3	115°	0.01	159.8	77.5	1.1
8	Octagonal	60°	2.88	57°	0.53	1.98	115°	0.01	121.3	50.2	0.9
9	Rectangular	60°	4.18	57°	0.48	2.16	140°	0.1	236.6	93.7	1.3
10	Circular	90°	3.08	90°	0.48	1.98	165°	0.13	137.7	68.2	1
11	Elliptical	90°	3.54	87°	0.53	1.52	132°	0.18	126.5	48.8	1.1
12	Jou.sharp	90°	2.44	87°	0.53	1.66	133°	0.03	64.5	52.3	0.8
13	Jou.round	90°	3.68	87°	0.5	1.88	160°	0.13	149.9	76.8	1.2
14	Oblong	90°	3.32	87°	0.5	1.7	135°	0.18	148.6	53.4	1.1
15	Sharpnose	90°	3.6	87°	0.5	1.56	130°	0.15	133.7	45.4	1.2
16	Hexagonal	90°	4.12	87°	0.53	1.86	123°	0.23	180.2	48.1	1.3
17	Octagonal	90°	3.56	87°	0.53	1.56	128°	0.01	134.5	56.5	1.2
18	Rectangular	90°	4.22	87°	0.48	1.9	135°	0.18	211.7	60	1.4
19	Circular	120°	2.68	119°	0.5	1.34	170°	0.05	64.6	34.9	1
20	Elliptical	120°	3.22	117°	0.5	1.6	60°	0.01	74.1	32.8	1.2
21	Jou.sharp	120°	2.12	123°	0.53	1.38	80°	0.03	30.6	31.4	0.8
22	Jou.round	120°	3.12	117°	0.53	1.62	65°	0.01	80.1	34.2	1.2
23	Oblong	120°	3.08	117°	0.48	1.7	60°	0.01	82.5	36.3	1.1
24	Sharpnose	120°	3.12	117°	0.5	1.5	50°	0.01	83.1	34.9	1.2
25	Hexagonal	120°	3.54	117°	0.5	1.62	60°	0.01	103.1	33.5	1.3
26	Octagonal	120°	3.24	117°	0.53	1.78	73°	0.01	87.1	37	1.2
27	Rectangular	120°	3.7	117°	0.48	1.72	174°	0.18	118.2	55.9	1.4

b distance from inner bank; *ds* = scour depth; *hs* sedimentation height; *V* scour hole volume; *Lms* length of sedimentation motion toward downstream

with a ratio of length to width equal to 5 implemented at the 60-degree, and the minimum equal to 47.7 times the third power of the pier width (V/D3 = 47.7) occurred with the oblong pier with a ratio of length to width equal to 2 installed at the 120-degree angle. Surfer software has been used for accurate drawing of shapes and calculation of scour hole volume. An example of this can be observed in Fig. 4. Figure 4a shows the bed topography around rectangular pier placed at 60-degree that has the maximum hole volume. Figure 4b shows the scour hole around the octagonal pier placed at 90-degree. Its volume is equal to 134.5 times the third power of the pier with ($V/D^3 = 134.5$) and Fig. 4c shows the scour hole around the jou.sharp pier placed at 120-degree that has the minimum hole volume.

As shown in Table 1, among the piers located at 60-degree angle of bend, the sediments around the octagonal pier had the lowest intrusion and the rectangular pier sediments had the highest downward intrusion and have moved to the downward up to 50.2 (*L*ms/*D* = 50.2) and 93.7 times the pier width (*L*ms/*D* = 93.7). At the angle of 90-degree, the sediments around the sharpnose pier with move up to 45.4 times the pier width toward the downstream (*L*ms/*D* = 45.4) have had the lowest motion, and the sediments around the jou.round pier with the value of 76.8 times the pier width (*L*ms/*D* = 76.8) have had the highest motion. In the case of the pier placement at 120-degree angle, the sediments around the jou.sharp and rectangular piers with the downstream intrusion up to 31.4 (*L*ms/*D* = 31.4) and 55.9 times the pier width (*L*ms/*D* = 55.9) have had the lowest and highest motion, respectively.

In the column related to the shape factor (*K*s) in Table 1, the ratio of maximum scour depth of each pier to the maximum scour depth around the circular pier is computed. As observed, the value of Ks is mostly affected by the pier geometric shape and the influence of position of the piers is small. For example, the shape factor for the jou.sharp pier at

all three angles was 0.8 and the shape factor for oblong pier was 1.1 at all three angles and showed similar performance in all three angles. The minimum and maximum shape factors in each of the three positions are, respectively, related to jou.sharp and rectangular piers. It is also in agreement with previous studies in straight channels that in all of them, rectangular pier has the highest shape factor value (Diab 2011).

The average maximum scour depth for the piers placement at 90-degree is maximum and at 120-degree is minimum. The mean scour depth for the pier placement at the angle of 120-degree compared to the angle of 60-degree is about 5.2 percent lower and compared to the placement angle of 90-degree has decreased by about 12%. It is also found that getting away from the beginning of the bend, the height of the sediments has decreased. So that the mean maximum sediment heights in the pier placement at the angle of 120-degree compared with the placement at the angle of 60-degree decreased by about 22 percent and decreased by 9.2 percent relative to the placement at 90-degree. In Table 1, the descending trend of the hole volume is seen by taking distance from the beginning of the bend. The mean scour hole volume in the pier placement at the angle of 120-degree compared to the placement at the angle of 60-degree decreased by about 46.8 percent and has decreased by about 43.8 percent relative to the placement at 90-degree. Also, for the pier placement at the angle of 120-degree, the mean intrusion of the sediments compared to the 60-degree placement decreased by 46.8 and, about 35 percent compared to the 90-degree placement.

Table 2 has provided the slope of scour holes in four directions. As observed, the maximum slope toward the inner bank is equal to 0.57 and for the placement mode of the circular pier at 90 degrees, the highest slope toward the outer bank is equal to 0.63 for rectangular pier at 60 degrees, the highest slope toward the upstream is 0.78 and in the case of circular pier at 120 degrees and the maximum slope toward the downstream hand is equal to 0.47 for the elliptical pier placed at an angle of 120 degrees. Also, according to the table, for all piers, as the position of the pier is approaching the end of the bend, the hole slope toward the downstream has increased.

In Fig. 5 the topographic changes of the channel bed have been provided for all piers placed at the angle of 60-degree. This figure shows that in all cases, the adjacent sedimentation of the inner bank is started at angle of 30-degree, which is due to the movement of transverse flows near the bed toward the bank that moves the material from the outer bank toward the inner bank.

Figure 5a, b, and c shows that the shape of the bed around circular, jou.round, and oblong piers with rounded nose are roughly the same. The materials around these piers have moved up to the end of the bend, and in all, the secondary scour hole has been created around 170-degree. However, given that the oblong pier has higher cross section compared to the jou.round pier and is symmetrical, the scour hole created around this pier has continued to the angle of about 90-degree. But around the jou.round pier, due to the sharp tip of the downstream nose and lower cross-sectional area, the turbulence of the stream near the upstream nose of the pier has been higher (according to qualitative flow pattern and experimental observations) and the scour hole has higher extension in the width compared to length and has extended to the outer bank.

Figure 5d, e, and f shows the topography of the bed around the elliptical, jou.sharp, and sharpnose pier. The separation of the flow around these three piers occurs due to the sharp nose very slow and gradually and, as shown in the figure, the bed around these piers has less variation than other piers, and the sediments have intrusion up to around 150-degree. But due to the fact that the nose of the elliptical pier is wider than the other two, the scour hole around this pier is more elongated toward the outer bank. But the jou. sharp and sharpnose piers do not divert flow to the edges due to their sharp nose. This causes the scour hole created around them to have smaller intrusion in width but moves further downward.

Figures 5g, h, and i show the topography of the bed around the hexagonal, octagonal, and rectangular piers. The nose of these three piers is wider than other piers. For this reason, as seen in the figure, the scour hole created around the hexagonal and rectangular piers covers a large width of the channel. But the octagonal pier is more aerodynamic compared to the rectangular pier, thus creates scour hole with smaller width and the surrounding sediments have lower intrusion toward downstream. The rectangular pier exhibits higher resistance to flow, due to the sharp edges its nose, and this results in a large scour hole and a high intrusion of the materials around the pier to the downstream direction.

In Fig. 6 the topographic changes of the channel bed have been provided for all piers placed at the angle of 90-degree. Figure 6a, b, and c shows bed changes around the circular, jou.round, and oblong piers. As shown in Fig. 6a, the materials around the circular pier has high intrusion toward downstream and have moved until the early downstream straight path.

With respect to Fig. 6b, it is observed that the materials around the jou.round pier due to the greater cross-sectional area of the pier than the circular pier, as well as the asymmetry of the section shape of this pier, have a large intrusion in the downstream direction and have entered the downstream straight path. According to Fig. 6a and b, due to the high volume of sedimentation on downstream of the pier and the passage of water from these sediments, two secondary scour holes were created at angles of 170- and 180-degree. However, in Fig. 6c, the materials around the oblong pier due

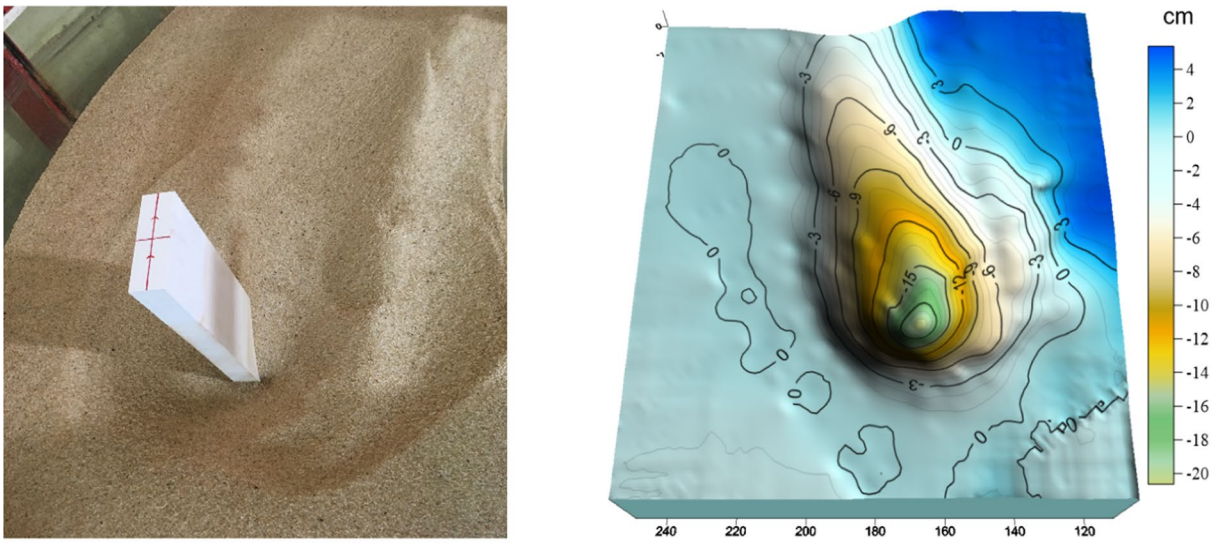
cm
4
2
0
-2
-4
-6
-8
-10
-12
-14
-16
-18
-20
240
220
200
180
160
140
120

(a)

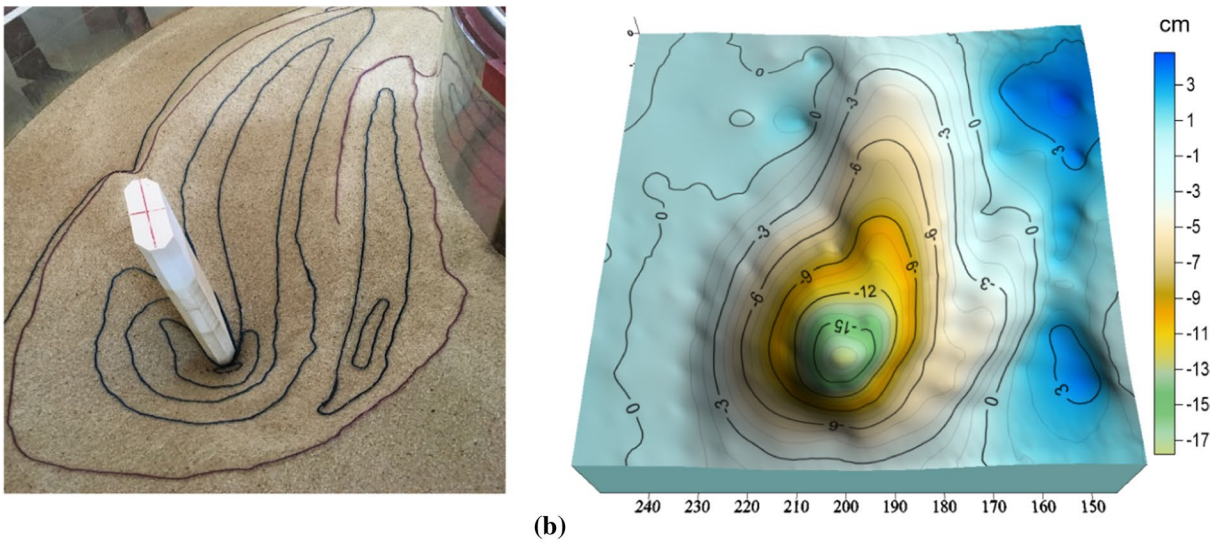
cm
3
1
-1
-3
-5
-7
-9
-11
-13
-15
-17
240
230
220
210
200
190
180
170
160
150

(b)

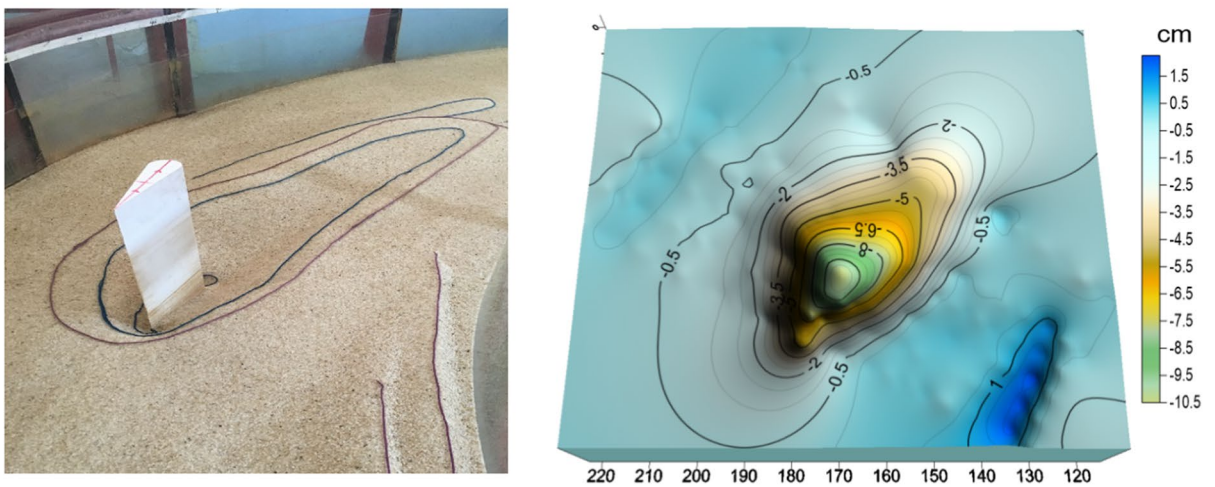
cm
1.5
0.5
-0.5
-1.5
-2.5
-3.5
-4.5
-5.5
-6.5
-7.5
-8.5
-9.5
-10.5
220
210
200
190
180
170
160
150
140
130
120

(c)

◂**Fig. 4** The scour hole created around **a** the rectangular pier located at the angle of 60-degree **b** an octagonal pier placed at the angle of 90-degree **c** a jou.sharp pier placed at the angle of 120-degree

to the symmetry of the section shape of this pier have had lower intrusion than the other two and have advanced to the end of the bend. Also, only one secondary scour hole is seen on the downstream of this pier.

Figure 6d, e, and f shows the topography of the bed around elliptical, jou.sharp, and sharpnose piers. The topographic changes around these three piers are very close to each other due to the same nose shape. The sediments around each of these three piers have relatively small intrusion and the secondary scour hole can be observed on the downstream of each pier, and at the 150-degree angle. According to Fig. 6e, no sedimentation occurred at the angle interval of 90- to 100-degree of the bend and adjacent to the inner bank. In explaining the cause of this phenomenon, it can be said that due to the rounded downstream nose of the jou.sharp pier, the flow in this area is more directed to the sides and prevents the sedimentation of the adjacent inner bank in this range.

Figure 6g, h, and i shows bed changes around the hexagonal, octagonal, and rectangular piers. Considering Fig. 6i, it can be seen that the rectangular pier, due to higher area of the cross section than two octagonal and hexagonal piers, creates larger scour hole and sedimentation with higher volume.

In Fig. 7 the topographic changes of the channel bed have been provided for all piers placed at the angle of 120-degree. According to Fig. 7, the changes of bed topography in the pier placement at the angle of 120-degree are very lower than the placement at the angles of 60- and 90-degree. The reason for this can be the effect of the downstream straight path.

According to Figs. 7a and i it is observed that, in the case of placement circular and rectangular piers, the maximum sedimentary height is associated with the angle of 170- and 174-degree, respectively, at the pier downstream. While in other piers, the maximum sedimentation height is at the pier

Table 2 slope of scour holes

No.	Pier's shape	position	I.S	O.S	U.S	D.S
1	Circular	60°	0.52	0.5	0.64	0.15
2	Elliptical	60°	0.45	0.55	0.57	0.12
3	Jou.sharp	60°	0.5	0.59	0.29	0.08
4	Jou.round	60°	0.42	0.42	0.5	0.07
5	Oblong	60°	0.45	0.57	0.63	0.11
6	Sharpnose	60°	0.42	0.58	0.67	0.07
7	Hexagonal	60°	0.39	0.44	0.62	0.14
8	Octagonal	60°	0.36	0.59	0.49	0.08
9	Rectangular	60°	0.48	0.63	0.59	0.18
10	Circular	90°	0.57	0.43	0.64	0.18
11	Elliptical	90°	0.46	0.59	0.59	0.23
12	Jou.sharp	90°	0.48	0.55	0.64	0.12
13	Jou.round	90°	0.45	0.53	0.57	0.22
14	Oblong	90°	0.45	0.47	0.58	0.2
15	Sharpnose	90°	0.51	0.61	0.63	0.24
16	Hexagonal	90°	0.54	0.54	0.65	0.29
17	Octagonal	90°	0.43	0.6	0.63	0.23
18	Rectangular	90°	0.56	0.53	0.59	0.29
19	Circular	120°	0.54	0.47	0.78	0.22
20	Elliptical	120°	0.48	0.53	0.65	0.47
21	Jou.sharp	120°	0.45	0.51	0.25	0.27
22	Jou.round	120°	0.42	0.47	0.54	0.39
23	Oblong	120°	0.45	0.44	0.52	0.35
24	Sharpnose	120°	0.46	0.48	0.63	0.37
25	Hexagonal	120°	0.45	0.57	0.62	0.38
26	Octagonal	120°	0.46	0.5	0.54	0.38
27	Rectangular	120°	0.46	0.51	0.63	0.35

I.S slope of hole toward the inner bank; *O.S* slope of hole toward the outer bank; *U.S* slope of hole toward upstream; *D,S* slope of hole toward downstream

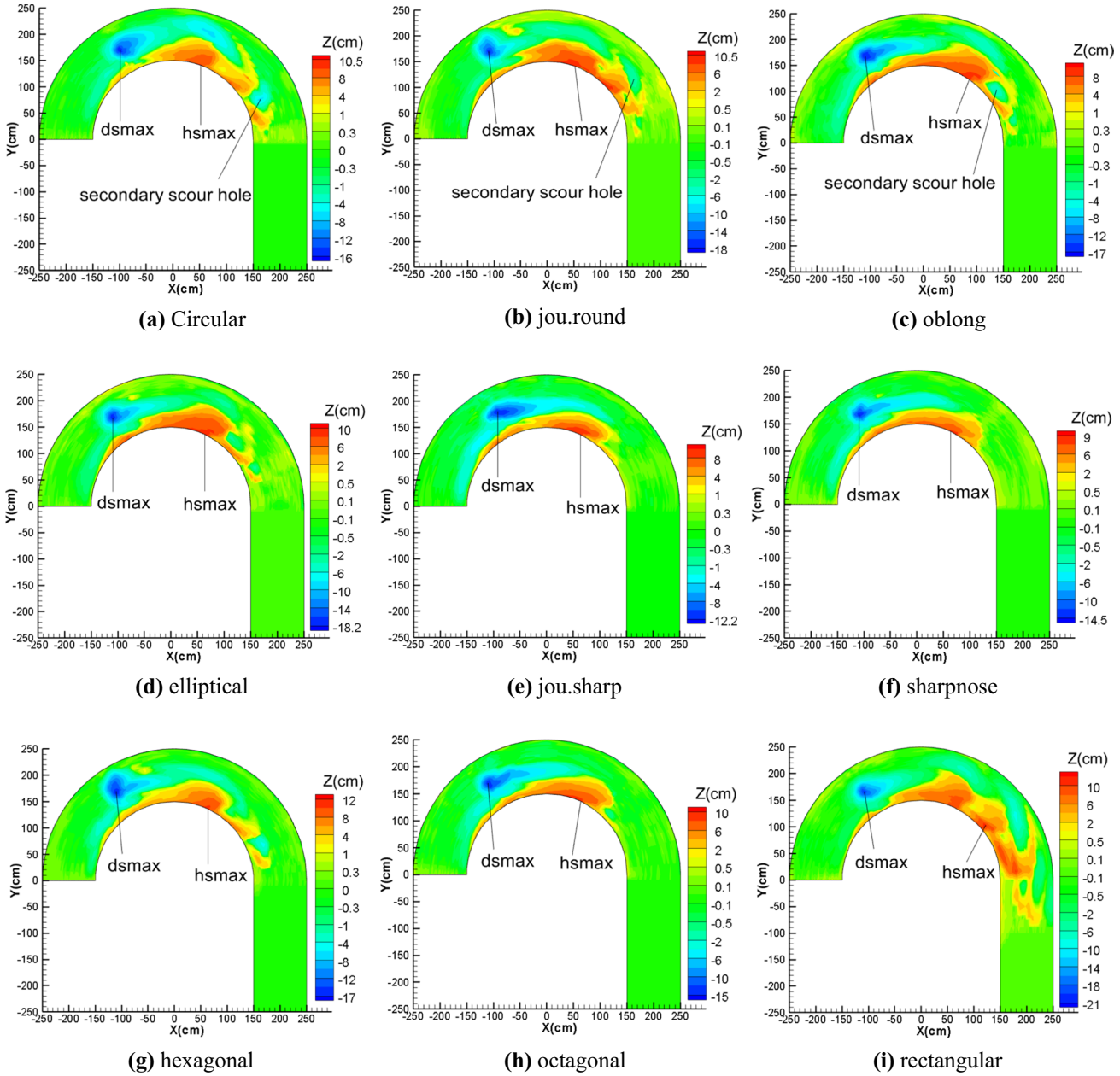

(a) Circular **(b)** jou.round **(c)** oblong

(d) elliptical **(e)** jou.sharp **(f)** sharpnose

(g) hexagonal **(h)** octagonal **(i)** rectangular

Fig. 5 Topographic changes of bed in the testing pier at the angle of 60-degree

upstream and around the angle of 50- to 80-degree adjacent to the inner bank. The formation of sedimentary ripples on the upstream of the pier and adjacent to the inner bank is further influenced by secondary flows and their combination with longitudinal flow and formation of spiral streams, while the formation of sedimentary ripples on the pier downstream is further affected by vortices caused by the collision of stream with pier. Therefore, it can be concluded that in the case of pier placement at an angle of 120-degree, for all piers except for the circular and rectangular piers, the effects of secondary flows are greater than the vortices resulting from the collision of the flow to the pier.

As shown in Fig. 7e and i, the jou.sharp and rectangular pier, due to their nose geometry, have produced the lowest and maximum changes in bed topography, respectively, while the materials surrounding the rectangular pier have entered the downstream straight path. In other piers, the changes are approximately the same, and after the sedimentary ripple formed at about 140- to 160-degree, a secondary scour hole has been formed around 170-degree.

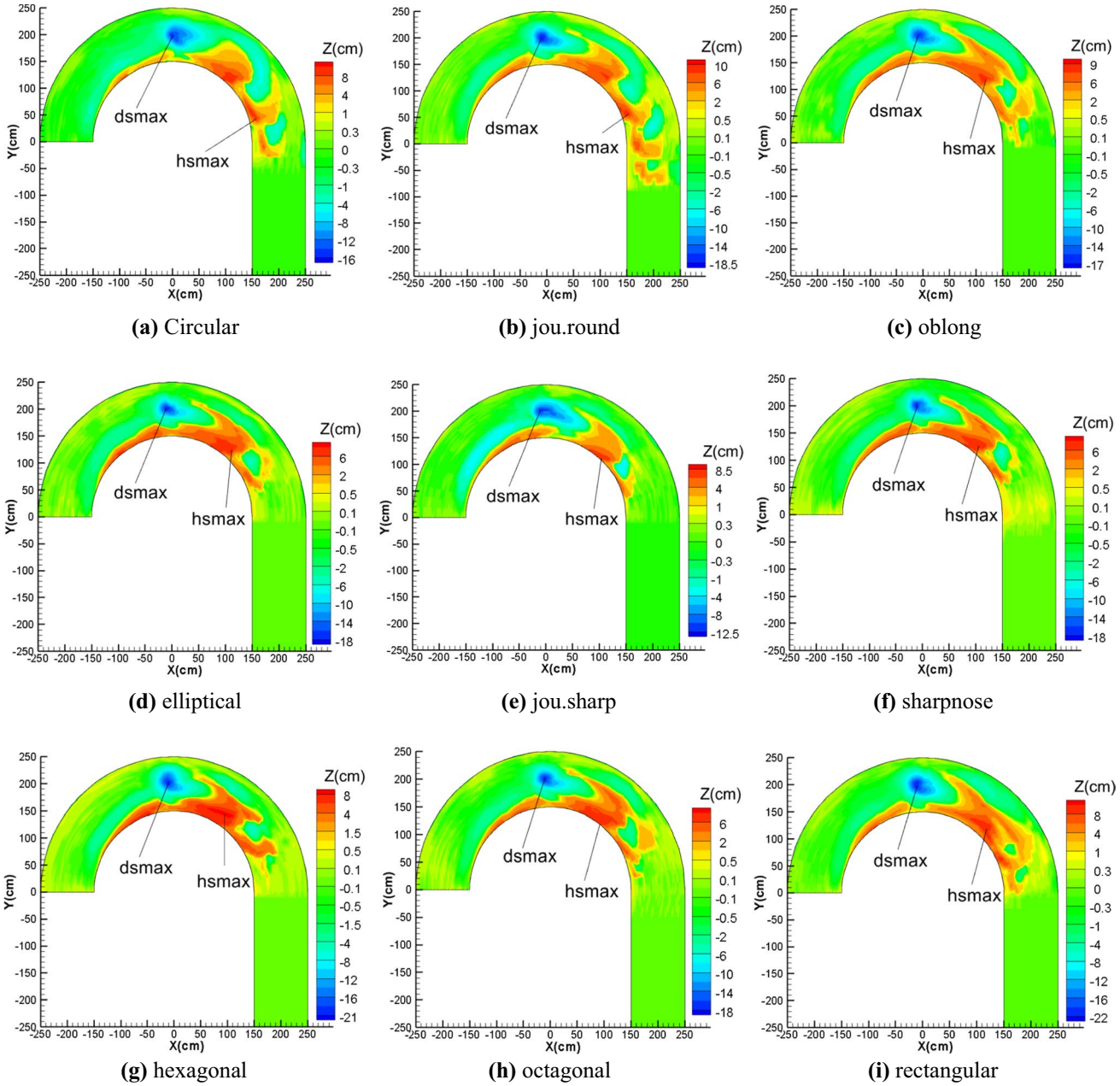

(a) Circular **(b)** jou.round **(c)** oblong

(d) elliptical **(e)** jou.sharp **(f)** sharpnose

(g) hexagonal **(h)** octagonal **(i)** rectangular

Fig. 6 Changes of bed topography in the test of pier placed at the angle of 90-degree

Figure 8 shows the time variation of the maximum scour depth, where the longitudinal axis is time in minutes and its lateral axis is the maximum depth of the scour hole nondimensionalized with the pier width. This figure shows that around the rectangular pier, the maximum hole depth formed at all three placement angles of 60-, 90- and 120-degree was larger compared to the other piers. This is because of the type of geometry and the sharp corner that strengthens the downflow of the pier front leading to deeper scours in total test time compared to the other piers.

According to Fig. 8a, among the piers placed at the angle of 60-degree of bend, for most of the duration of the experiment, except for the interval of 46–59 percent of the relative equilibrium time, the lowest scouring was created around the jou.sharp pier. But during the time period of 46–59 percent of the relative equilibrium time, the sharpnose pier had the lowest scour. It is conjectured that this is because the jou. sharp and sharpnose piers create less flow separation and turbulence, due to the sharpness of their nose and the aerodynamic shape of these piers. Also, in Fig. 8a, the scour

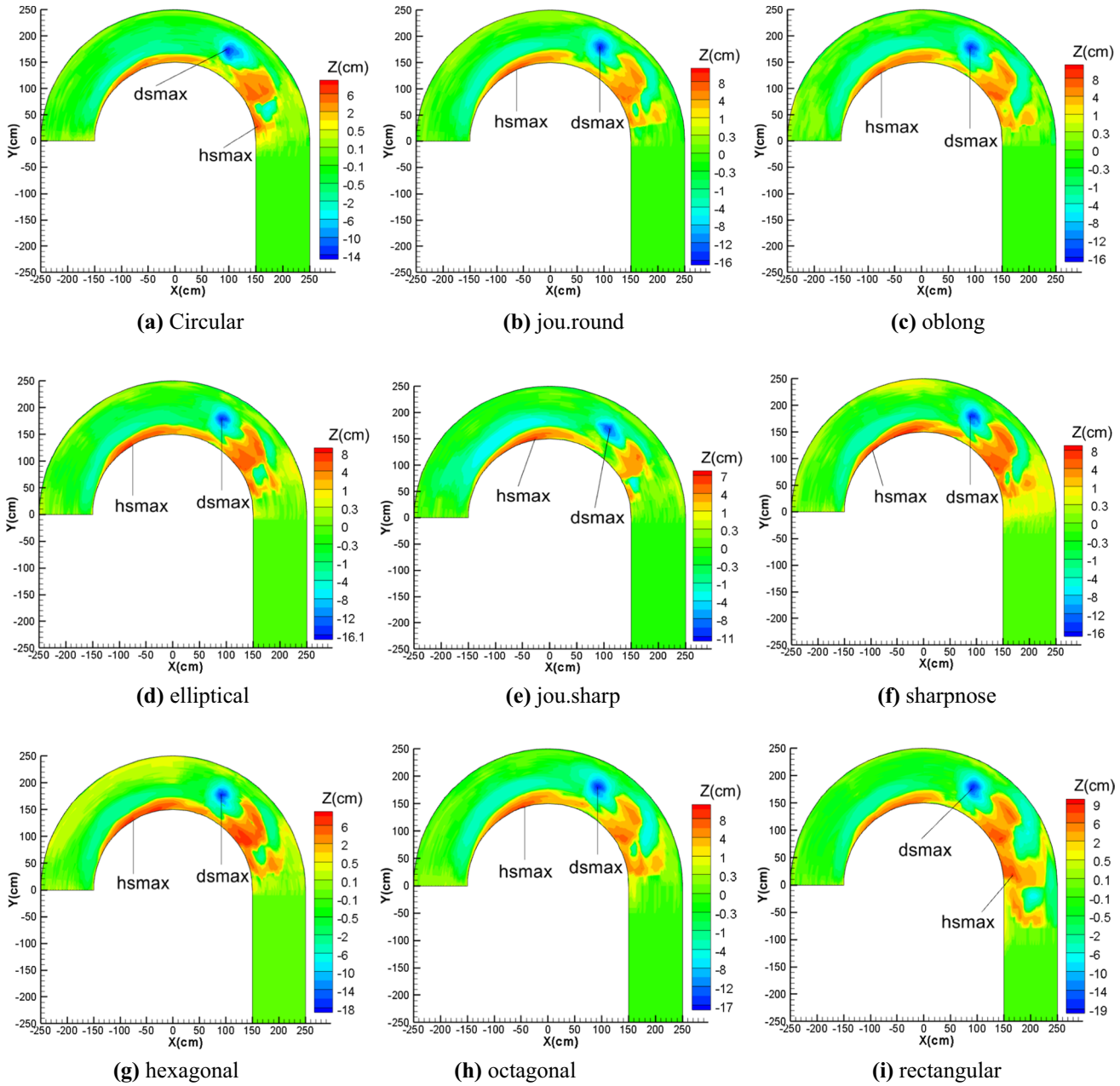

Fig. 7 Changes of bed topography in testing piers placed at the angle of 120-degree

depth of the hexagonal pier curve in the range of 52–72 percent of the relative equilibrium time shows a decreasing and then an increased trend that continues to the end of the experiment.

In the case of the jou.sharp pier, unlike other piers, scour around the downstream nose is higher than the upstream nose due to the sharp tip of the nose upstream and the rounded downstream nose and the difference in the flow pattern around it. Therefore, according to Fig. 8a, after passing 30% of the test time and according to Fig. 8c, after 52% of the test time, some of the sediments transported from the upstream nose were transferred to the downstream hole and reduced the hole depth in part of the time intervals of the test.

As shown in Fig. 8b, for some piers, at a period of approximately 20% of the time of the experiment, the slope of the graph suddenly increased. For example, the curves for the elliptical, jou.sharp and octagonal piers, after 22 percent of the time and for hexagonal and sharpnose piers, after 26 percent of the duration of the experiment, sharp slope changes

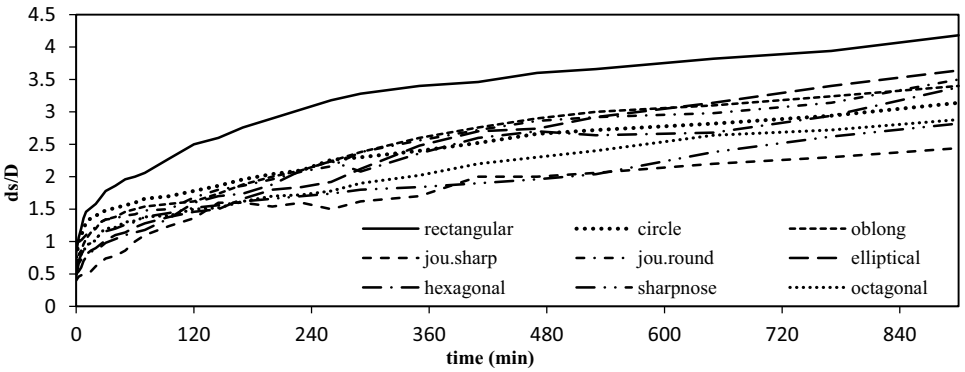

Fig. 8 Maximum scour depth with time in the pier placement at angles of **a** 60-degree **b** 90-degree **c** 120-degree

are observed. As the volume of the scour hole around the pier increases, the intensity of the vortices created inside the hole also increases and causes further increase of the hole depth. It is also seen that for oblong and circular piers there is no sudden jump in the maximum scour depth variation in their curves, despite the differences in their nose geometry.

According to Fig. 8c, the graphs associated with the maximum scour depth of piers located at 120-degree are steadily increasing with a slight slope, and only in the case of hexagonal pier, a sudden slope change can be observed after 46% of the experiment time.

Figure 9 shows examples of transverse sections of the scour adjacent to the upstream nose of the piers at the placement angles of 60-, 90-, and 120-degree. As shown in the figure, under the influence of the spiral flows created in the bend, sedimentation occurs adjacent to the inner bank. The height of these sediments at the placement angle of 60-degree is higher than those the angle of 90- and 120-degree.

According to Fig. 9a, the maximum sedimentation height adjacent to the inner bank at the angle of 60-degree corresponds to the elliptical pier and is 1.52 times the pier width. Also, according to Fig. 9b, the maximum

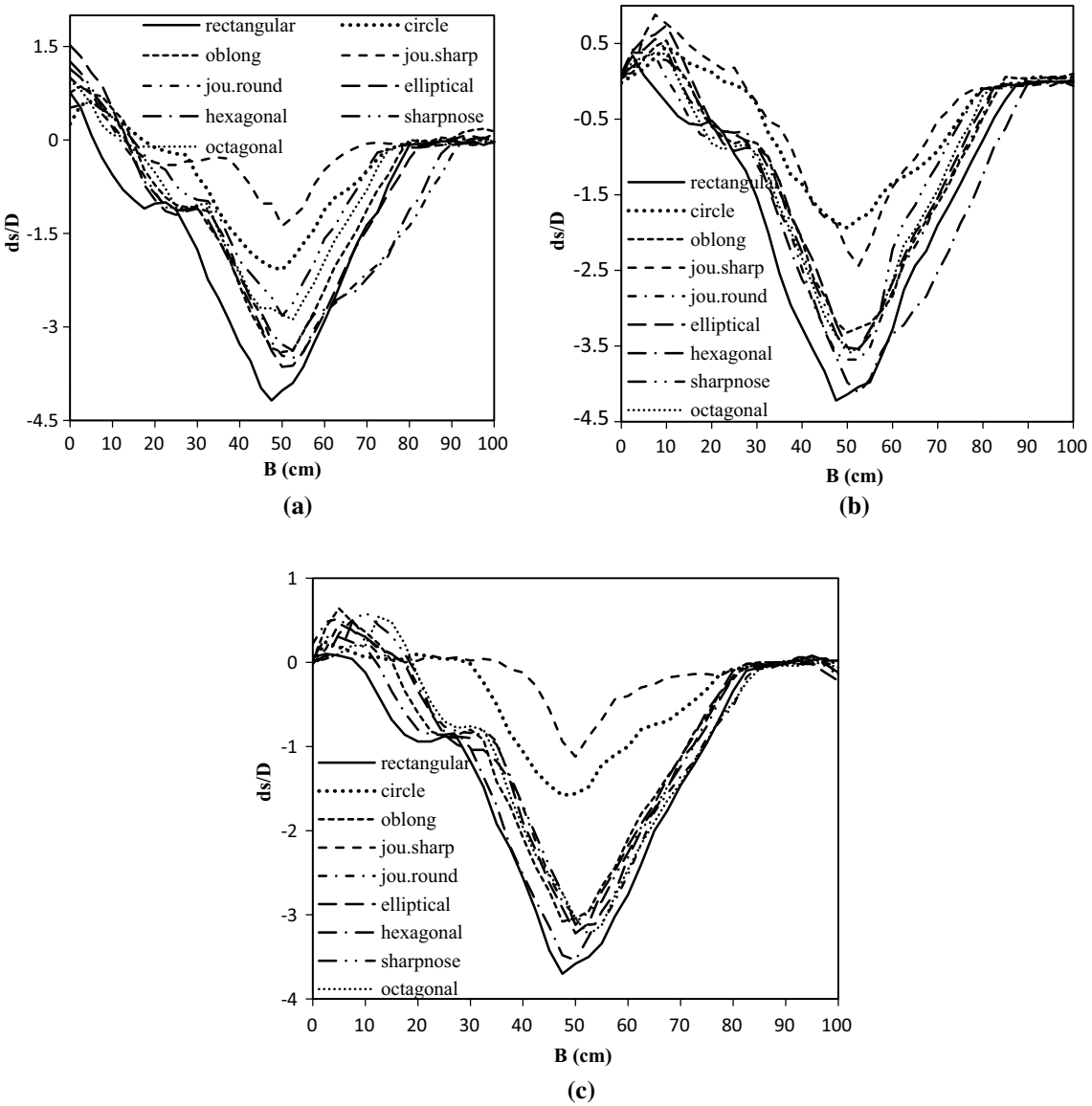

Fig. 9 Examples of transverse sections of the scour adjacent to the upstream nose of the piers at the placement angles of **a** 60-degree **b** 90-degree **c** 120-degree

sedimentation height is related to the jou.sharp pier placement and is 0.88 times the pier width at the distance of 7.5% of the channel width from the inner bank. The lower deviation of the flow toward the inner bank around these two piers leads to higher sedimentation adjacent to the inner bank and decrease the hole width. According to Fig. 9, it is obvious that at all three placement angles, the jou.sharp pier has created holes with very low width near its nose due to creation of low flow separation. In contrast, piers with high nose widths make their holes wider. For this reason, as shown in Fig. 9a and b, the scour hole created around the rectangular pier starts at about 10% of the channel width from the inner bank and the hole around the hexagonal pier extends to about 85% of the channel width toward the outer bank and creates wider holes.

Figure 9c shows that with the placement of piers at the angle of 120-degree, due to the closeness to the downstream straight path, the height of the sedimentary ripples adjacent to the inner bank and the depth of the scour holes are decreased. The maximum height of these ripples is only 64 percent of the pier width and occurred at a distance of 5% of the channel width from the inner bank and is related to the oblong pier placement.

Figure 10 shows an example of longitudinal sections at the center of the channel at the three placement angles. As described in Table 2, the longitudinal slope of the hole on

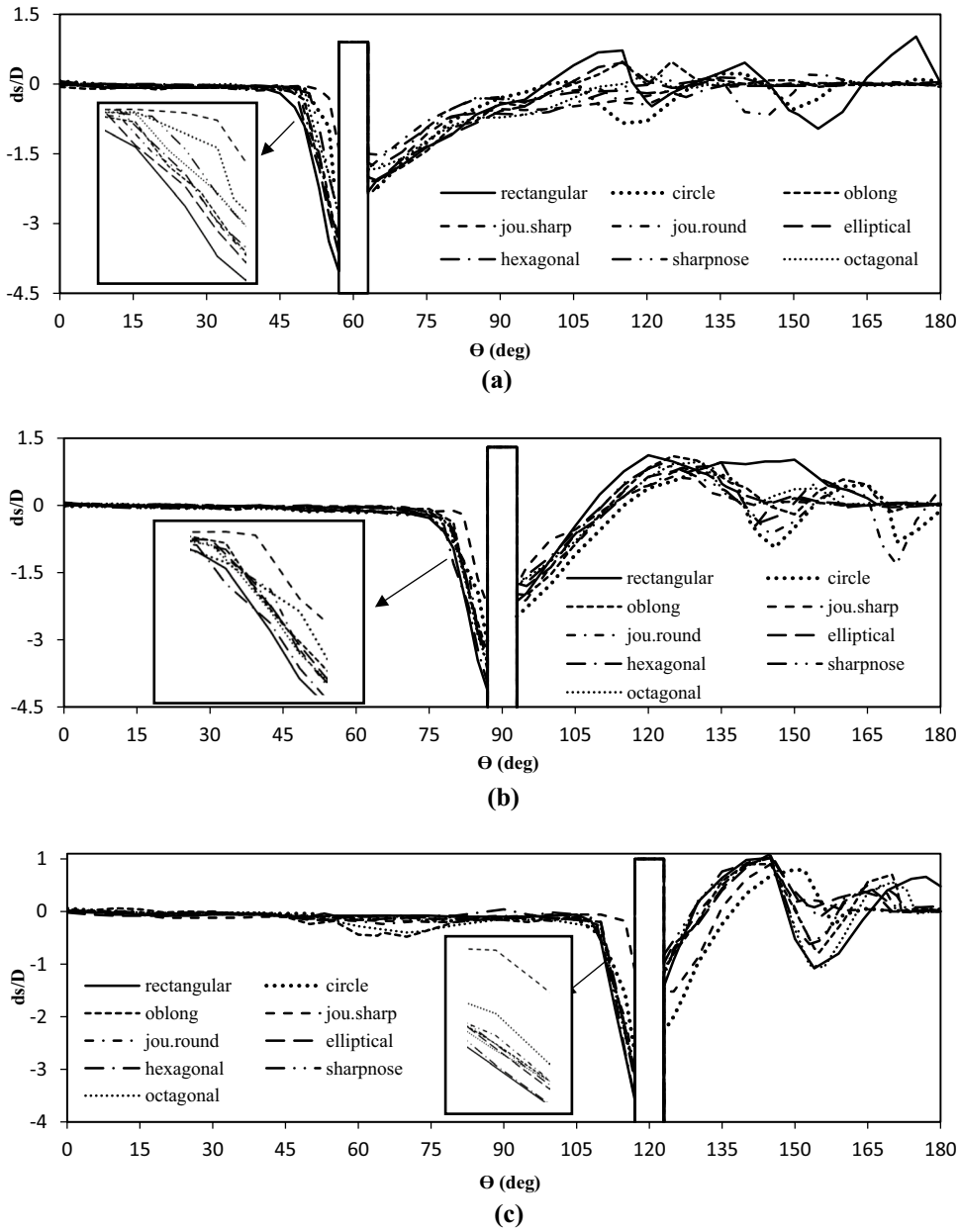

Fig. 10 Examples of a longitudinal sections of the scour at the center of the channel in the case of pier placement at the angles of **a** 60-degree **b** 90-degree **c** 120-degree

the downstream of the pier is the lowest for the 60-degree piers and maximum for the 120-degree piers. This indicates that the power of the horseshoe vortices behind the pier, which moves the materials down, is higher at 60-degree, and as the pier placement position approaches to the end of the bend, the power of the vortices decreases. This observation is also in agreement with the laboratory results of Vaghefi et al. (2016), which states that the maximum amount of vorticity (cell rotation amount) and shear stress occur near the bed at the 40- to 60-degree interval.

It is also seen in Fig. 10 that, at all three placement angles, the hole formed around the jou.sharp pier has the lowest intrusion in the pier upstream and has a significant difference compared with other piers. This is due to the fact that, considering the specific geometry of the nose of jou. sharp pier, as flow collides with the nose of this pier, downflows with lower power are formed relative to other piers with a higher nose section and causes the scour hole around this pier has a lower stretch to the upstream.

According to Fig. 10, the materials removed from the pier surrounding were transferred downstream by the flow and formed sedimentary ripples. Then, due to the passage of water from these ripples and a sudden downturn on the downstream bed, secondary scour holes are created.

Figure 11 shows the rectangular surrounding the scour holes in all experiments at each of the 60, 90, and

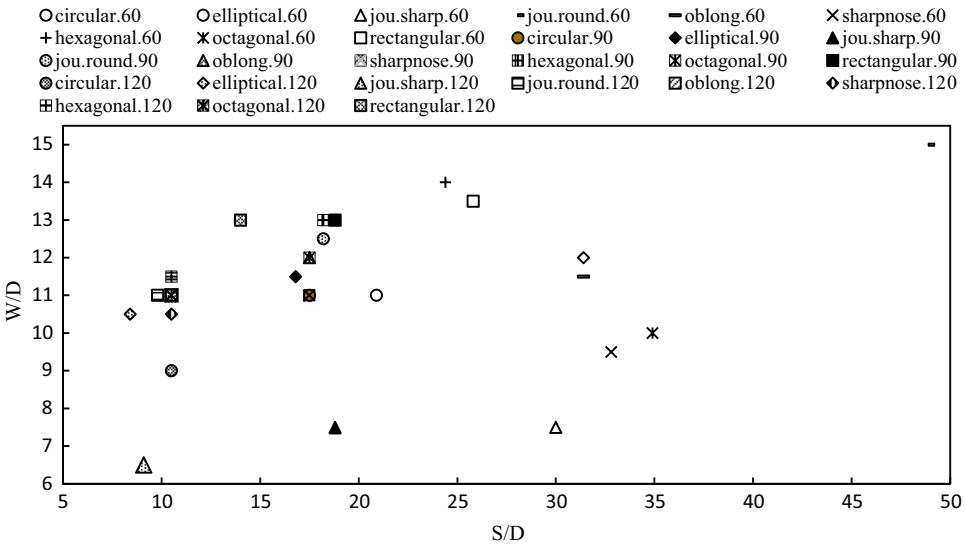

Fig. 11 Nondimensionalized dimensions of the surrounded rectangle to scour holes

120-degree placement of the bend. The longitudinal axis of this diagram is the maximum length of the scour hole (S) nondimensionalized with the pier width and its lateral axis is the maximum width of the scour hole (W) nondimensionalized with the pier width. It is observed that, among all the experiments, the hole created around the jou.round pier placed at the angle of 60-degree with a length equal to 48.9 times the pier width and the width equal to 15 times the pier width is considered as the largest hole (Fig. 12a). It is observed that the hole created around the octagonal pier placed at 60-degree with a length equal to 34.9 times the pier width has the largest length and the hexagonal pier placed at the 60-degree with a width equal to 14 times the pier width has the largest width after the jou.round pier placed at 60-degree.

In contrast, the hole created around the jou.sharp pier located at the angle of 120-degree of the bend with a width equal to 6.5 times the pier width, has the lowest width and the hole created around the elliptical pier located at the angle of 120-degree with a length equal to 8.4 times the pier width, and has the lowest length among other holes (Fig. 12b).

4 Conclusion

In this study the effects of the shape and position of the pier placement on the changes of bed topography in a 180-degree bend were investigate. The results showed that with decreasing nose width and sharpening it, the depth and volume of the scour hole was decreased. Among the experiments, the minimum and maximum scour depth was observed for the jou.sharp pier placed at the angle of 120-degree and the rectangular pier placed at the angle of 90-degree, which were equal to 2.12 and 4.22 times the pier width, respectively. The maximum sedimentation height is 2.3 times the pier width on the downstream of the hexagonal pier, placed at the angle of 60-degree adjacent to the inner bank at the angle of 115-degree of the bend. The materials around the rectangular pier placed at 60-degree have had the highest intrusion and are 93.7 times of the pier width downward. Also, it was found that with the placement of the piers at 120-degree, the average volume of the holes created was about 46.8 percent lower than those at the 60-degree and about 43.8 percent lower than those at the 90-degree.

The presented results also showed that the shape factor (Ks) was mostly affected by the pier geometric shape and the influence of position of the piers was small. The minimum and maximum shape factors in each of the three positions were, respectively, for the jou.sharp and rectangular piers. The shape factor for the jou.sharp pier at all three angles was 0.8 and the shape factor for oblong pier was 1.1 at all three angles. Thus, the jou.sharp and oblong piers showed similar performance in all three angles.

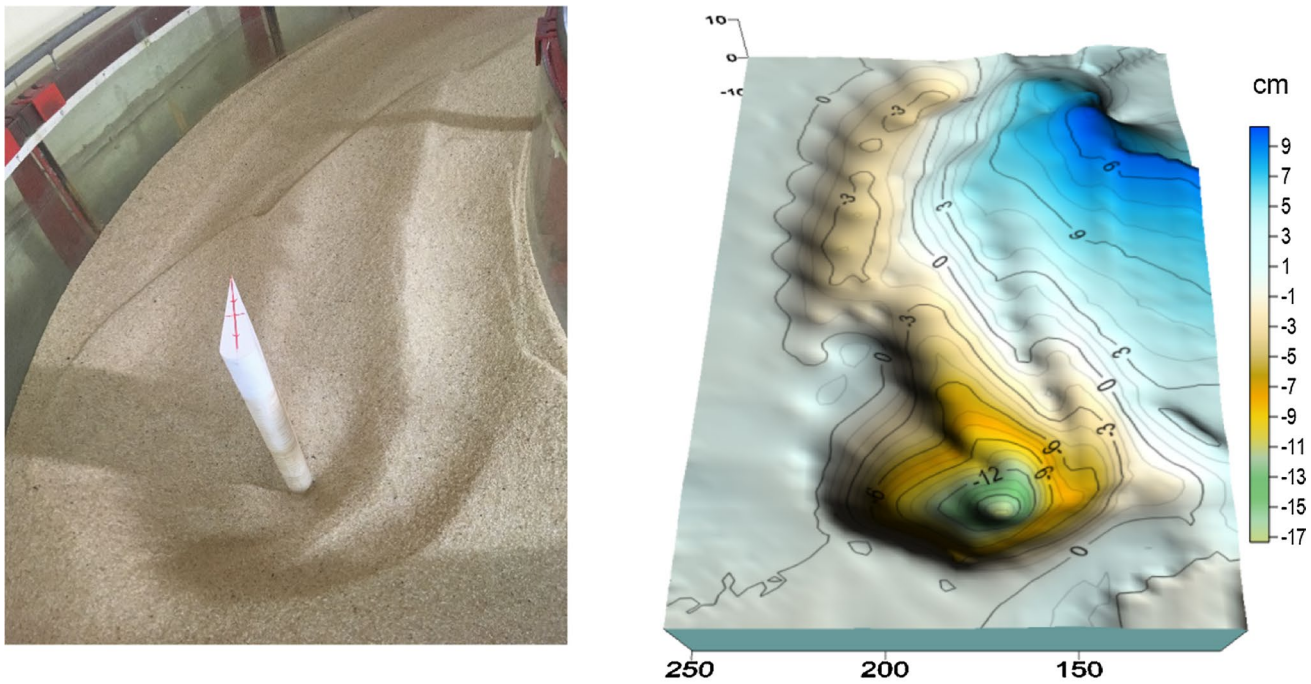

(a)

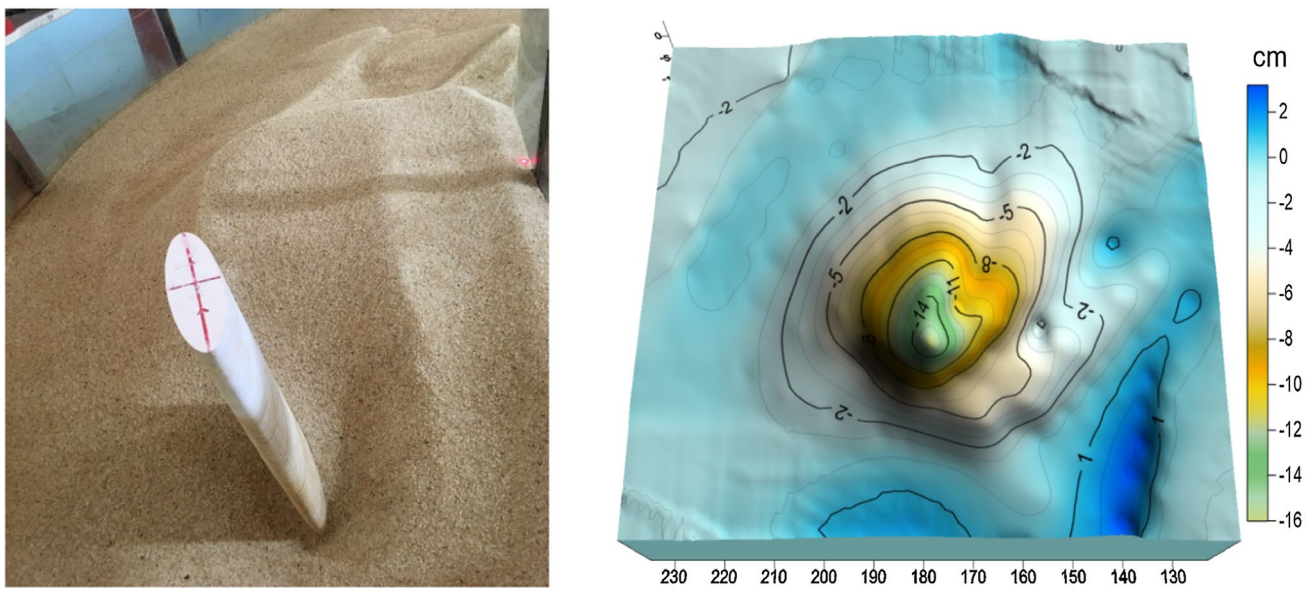

(b)

Fig. 12 The scour hole created around **a** The jou.round pier place at the angle of 60-degree **b** The elliptical pier place at the angle of 120-degree

References

Akib S, Jahangirzadeh A, Basser H (2014) Local scour around complex pier groups and combined piles at semi-integral bridge. J Hydrol Hydromech 62(2):108–116. https://doi.org/10.2478/johh-2014-0015

Al-Shukur AHK, Obeid ZH (2016) Experimental study of bridge pier shape to minimize local scour. Int J Civil Eng Technol 7(1):162–171

Baghbadorani DA, Beheshti AA, Ataie-Ashtiani B (2017) Scour hole depth prediction around pile groups: review, comparison of existing methods, and proposition of a new approach. Natural Haz 88(2):977–1001. https://doi.org/10.1007/s11069-017-2900-9

Ben Mohammad Khajeh S, Vaghefi M, Mahmoudi A (2017) The scour pattern around an inclined cylindrical pier in a sharp 180-degree bend: an experimental study. Int J River Basin Manage 15(2):207–218. https://doi.org/10.1080/15715124.2016.1274322

Carnacina I, Pagliara S, Leonardi N (2019) Bridge pier scour under pressure flow conditions. River Res Appl 35(7):844–854. https://doi.org/10.1002/rra.3451

Chavan R, Gualtieri P, Kumar B (2019) Turbulent flow structures and scour hole characteristics around circular bridge piers over non-uniform sand bed channels with downward seepage. Water 11(8):1580. https://doi.org/10.3390/w11081580

Chiew YM (1992) Scour protection at bridge piers. J Hydraulic Eng 118(9):1260–1269

Chiew YM, Melville BW (1987) Local scour around bridge piers. J Hydraulic Res 25(1):15–26. https://doi.org/10.1080/00221688709499285

Das R, Das S, Jaman H, Mazumdar A (2019) Impact of upstream bridge pier on the scouring around adjacent downstream bridge pier. Arab J Sci Eng 44(5):4359–4372. https://doi.org/10.1007/s13369-018-3418-5

Dehghan D, Vaghefi M, Ghodsian M (2021a) Experimental study of the effect of the length-to-width ratio and skewness angles of the pier installed at the bend on scour pattern. J Braz Soc Mech Sci Eng 43(3):1–17. https://doi.org/10.1007/s40430-021-02884-y

Dehghan D, Vaghefi M, Ghodsian M (2021b) The effect of collar width ratio on the flow pattern around oblong pier in bend. Water Supply. https://doi.org/10.2166/ws.2021.165

Diab RMAEA (2011) Experimental Investigation on scouring around piers of different shape and alignment in gravel. Doctoral dissertation, TU Darmstadt.

Fael C, Lança R, Cardoso A (2016) Effect of pier shape and pier alignment on the equilibrium scour depth at single piers. Int J Sediment Res 31(3):244–250. https://doi.org/10.1016/j.ijsrc.2016.04.001

Farooq R, Ghumman AR (2019) Impact assessment of pier shape and modifications on scouring around bridge pier. Water 11(9):1761. https://doi.org/10.3390/w11091761

Galan A, Simarro G, Fael C, Cardoso AH (2019) Clear-water scour at submerged pile groups. Int J River Basin Manage 17(1):101–108. https://doi.org/10.1080/15715124.2018.1446964

Ismael A, Gunal M, Hussein H (2015) Effect of bridge pier position on scour reduction according to flow direction. Arab J Sci Eng 40(6):1579–1590. https://doi.org/10.1007/s13369-015-1625-x

Karimaei Tabarestani M, Zarrati AR (2019) Local scour depth at a bridge pier protected by a collar in steady and unsteady flow. Proc Institution Civil Eng Water Manage 172 (6):301–311. https://doi.org/10.1680/jwama.18.00061

Keshavarzi A, Shrestha CK, Melville B, Khabbaz H, Ranjbar-Zahedani M, Ball J (2018) Estimation of maximum scour depths at upstream of front and rear piers for two in-line circular columns. Environ Fluid Mech 18(2):537–550. https://doi.org/10.1007/s10652-017-9572-6

Khaple S, Hanmaiahgari PR, Gaudio R, Dey S (2017) Interference of an upstream pier on local scour at downstream piers. Acta Geophys 65(1):29–46. https://doi.org/10.1007/s11600-017-0004-2

Laxmi Narayana P, Timbadiya PV, Patel PL (2020) Bed level variations around submerged tandem bridge piers in sand beds. ISH J Hydraulic Eng, pp 1–9. https://doi.org/10.1080/09715010.2020.1723138

Lee SO, Hong SH (2019) Turbulence characteristics before and after scour upstream of a scaled-down bridge pier model. Water 11(9):1900. https://doi.org/10.3390/w11091900

Link O, García M, Pizarro A, Alcayaga H, Palma S (2020) Local scour and sediment deposition at bridge piers during floods. J Hydraulic Eng 146(3):04020003. https://doi.org/10.1061/(ASCE)HY.1943-7900.0001696

Malik R, Setia B (2020) Interference between pier models and its effects on scour depth. SN Appl Sci 2(1):68. https://doi.org/10.1007/s42452-019-1868-3

Masjedi A, Bejestan MS, Kazemi H (2010) Effects of bridge pier position in a 180 degree flume bend on scour hole depth. J Appl Sci 10(8):670–675

Melville BW, Chiew YM (1999) Time scale for local scour at bridge piers. J Hydraulic Eng 125(1):59–65. https://doi.org/10.1061/(ASCE)0733-9429(1999)125:1(59)

Memar S, Zounemat-Kermani M, Beheshti A, Rahimpour M, De Cesare G, Schleiss AJ (2020) Influence of collars on reduction in scour depth at two piers in a tandem configuration. Acta Geophys 68(1):229–242. https://doi.org/10.1007/s11600-019-00393-0

Moghanloo M, Vaghefi M, Ghodsian M (2020a) Experimental study on the effect of thickness and level of the collar on the scour pattern in 180° sharp bend with bridge pier. Iran J Sci Technol Trans Civil Eng, pp 1–19. https://doi.org/10.1007/s40996-020-00511-9

Moghanloo M, Vaghefi M, Ghodsian M (2020b) Experimental investigation on the effect of increasing the collar thickness on the flow pattern around the oblong pier in 180° sharp bend with balanced bed. J Appl Fluid Mech (JAFM) 13(1):245–260. https://doi.org/10.29252/jafm.13.01.30164

Moreno M, Maia R, Couto L (2016) Effects of relative column width and pile-cap elevation on local scour depth around complex piers. J Hydraulic Eng 142(2):04015051. https://doi.org/10.1061/(ASCE)HY.1943-7900.0001080

Namaee MR, Sui J (2019) Local scour around two side-by-side cylindrical bridge piers under ice-covered conditions. Int J Sediment Res 34(4):355–367. https://doi.org/10.1016/j.ijsrc.2018.11.007

Tipireddy RT, Barkdoll BD (2019) Scour reduction by air injection at a cylindrical bridge pier: Experimental determination of optimal configuration. J Hydraulic Eng 145(1):06018016. https://doi.org/10.1061/(ASCE)HY.1943-7900.0001555

Vaghefi M, Akbari M, Fiouz AR (2016) An experimental study of mean and turbulent flow in a 180 degree sharp open channel bend: secondary flow and bed shear stress. KSCE J Civil Eng 20(4):1582–1593. https://doi.org/10.1007/s12205-015-1560-0

Vaghefi M, Motlagh MJTN, Hashemi SS, Moradi S (2018) Experimental study of bed topography variations due to placement of a triad series of vertical piers at different positions in a 180° bend. Arab J Geosci 11(5):102. https://doi.org/10.1007/s12517-018-3443-4

Vijayasree BA, Eldho TI, Mazumder BS, Ahmad N (2019) Influence of bridge pier shape on flow field and scour geometry. Int J River Basin Manage 17(1):109–129. https://doi.org/10.1080/15715124.2017.1394315

Wang H, Tang H, Liu Q, Wang Y (2016) Local scouring around twin bridge piers in open-channel flows. J Hydraulic Eng 142(9):06016008. https://doi.org/10.1061/(ASCE)HY.1943-7900.0001154

Wang L, Melville BW, Whittaker CN, Guan D (2018) Effects of a downstream submerged weir on local scour at bridge piers. J Hydro-Environment Res 20:101–109. https://doi.org/10.1016/j.jher.2018.06.001

Wang S, Wei K, Shen Z, Xiang Q (2019) Experimental investigation of local scour protection for cylindrical bridge piers using anti-scour collars. Water 11(7):1515. https://doi.org/10.3390/w11071515

Yagci O, Yildirim I, Celik MF, Kitsikoudis V, Duran Z, Kirca VO (2017) Clear water scour around a finite array of cylinders. Appl Ocean Res 68:114–129. https://doi.org/10.1016/j.apor.2017.08.014

Yang Y, Melville BW, Sheppard DM, Shamseldin AY (2018) Clear-water local scour at skewed complex bridge piers. J Hydraulic Eng 144(6):04018019. https://doi.org/10.1061/(ASCE)HY.1943-7900.0001458

Yang Y, Melville BW, Sheppard DM, Shamseldin AY (2019a) Live-bed scour at wide and long-skewed bridge piers in comparatively shallow water. J Hydraulic Eng 145(5):06019005. https://doi.org/10.1061/(ASCE)HY.1943-7900.0001600

Yang Y, Melville BW, Macky GH, Shamseldin AY (2019b) Local scour at complex bridge piers in close proximity under clear-water and live-bed flow regime. Water 11(8):1530. https://doi.org/10.3390/w11081530

Yang Y, Melville BW, Macky GH, Shamseldin AY (2020) Temporal evolution of clear-water local scour at aligned and skewed complex bridge piers. J Hydraulic Eng 146(4):04020026. https://doi.org/10.1061/(ASCE)HY.1943-7900.0001732